Chemistry & Biology
Article

XPF-Dependent DNA Breaks and RNA Polymerase II Arrest Induced by Antitumor DNA Interstrand Crosslinking-Mimetic Alkaloids

Sascha Feuerhahn,[1,5] Christophe Giraudon,[1,5] Marta Martínez-Díez,[2] Juan A. Bueren-Calabuig,[3] Carlos M. Galmarini,[2] Federico Gago,[3] and Jean-Marc Egly[1,4,*]
[1]Institut de Génétique et de Biologie Moléculaire et Cellulaire, CNRS/INSERM/UdS, BP 163, 67404 Illkirch Cedex, C. U. Strasbourg, France
[2]Cell Biology Department, PharmaMar, Avda. de los Reyes, 1 Pol. Ind. La Mina, 28770 Colmenar Viejo, Madrid, Spain
[3]Departmento de Farmacología, Universidad de Alcalá, E-28871 Alcalá de Henares, Madrid, Spain
[4]Institut de Recherche contre les Cancers de l'Appareil Digestif, 1 place de l'Hôpital, 67000 Strasbourg, France
[5]These authors contributed equally to this work
*Correspondence: egly@igbmc.fr
DOI 10.1016/j.chembiol.2011.06.007

SUMMARY

Trabectedin and Zalypsis are two potent anticancer tetrahydroisoquinoline alkaloids that can form a covalent bond with the amino group of a guanine in selected triplets of DNA duplexes and eventually give rise to double-strand breaks. Using well-defined in vitro and in vivo assays, we show that the resulting DNA adducts stimulate, in a concentration-dependent manner, cleavage by the XPF/ERCC1 nuclease on the strand opposite to that bonded by the drug. They also inhibit RNA synthesis by: (1) preventing binding of transcription factors like Sp1 to DNA, and (2) arresting elongating RNA polymerase II at the same nucleotide position regardless of the strand they are located on. Structural models provide a rationale for these findings and highlight the similarity between this type of DNA modification and an interstrand crosslink.

INTRODUCTION

One major challenge in cancer therapeutics is to characterize the altered biochemical pathway in the tumor cell that can be selectively targeted by drugs. Many clinically used antineoplastic agents cause DNA damage, and their action is influenced by their ability to specifically disturb fundamental DNA metabolic processes such as replication, repair, and transcription (Bustamante et al., 2011).

Trabectedin (Yondelis, ecteinascidin-743), a compound originally extracted from the marine tunicate *Ecteinascidia turbinata* (Rinehart et al., 1990) and commercially prepared nowadays by semisynthesis from microbially produced cyanosafracin (Cuevas and Francesch, 2009), and Zalypsis, a molecule structurally related to jorumycin and renieramycins (Scott and Williams, 2002), are two tetrahydroisoquinoline alkaloids (Figures 1A and 1B) endowed with potent anticancer activities. Trabectedin is currently used for the treatment of advanced soft tissue sarcoma and, in combination with pegylated liposomal doxorubicin, relapsed platinum-sensitive ovarian cancer (D'Incalci and Galmarini, 2010). Zalypsis is particularly effective against leukemia and stomach tumor cell lines (Leal et al., 2009), is in phase II clinical trials (Oku et al., 2003), and appears to be promising for the treatment of multiple myelomas (Ocio et al., 2009).

Both drugs bind covalently to the exocyclic 2 amino group of a central guanine (G) in selected triplet sequences of double-stranded DNA (dsDNA). Thus, the adducts are located in the DNA minor groove (Leal et al., 2009; Pommier et al., 1996; Zewail-Foote and Hurley, 1999), where the drugs also establish additional noncovalent interactions with the sugar-phosphate backbone and other nucleobases in both the strand containing the adduct (AS) and the complementary, opposite strand (OS), of the same duplex. As a result, the drug-induced lesion has been suggested to functionally mimic an interstrand crosslink (ICL), a type of DNA damage that is highly effective in blocking replication and transcription (Casado et al., 2008; De Silva et al., 2000). ICL resolution occurs through the coordinated action of multiple DNA repair pathways (McHugh et al., 2001), including nucleotide excision repair (NER) and homologous recombination (HR), in a process that involves double-strand breaks (DSBs). Interestingly, exposure of cells to trabectedin (Casado et al., 2008; Guirouilh-Barbat et al., 2008; Soares et al., 2007; Tavecchio et al., 2008) or Zalypsis (Guirouilh-Barbat et al., 2009; Leal et al., 2009; Ocio et al., 2009) results in the generation of DSBs, as assessed by γ-H2AX and Rad51 foci formation. Moreover, HR-deficient Fanconi anemia cells are extremely sensitive to trabectedin (Casado et al., 2008). On the contrary, trabectedin is more cytotoxic in NER-proficient cells than in their NER-deficient counterparts, particularly those harboring deficiencies in the XPG and XPF endonucleases, XPB helicase, and/or ERCC1, the partner of XPF (Damia et al., 2001; Takebayashi et al., 2001; Zewail-Foote et al., 2001). Furthermore, it was shown that pharmacological concentrations of trabectedin can inhibit expression of many NF-Y targeted genes including those encoding the multidrug resistance efflux pump MDR1 (Jin et al., 2000) and the molecular chaperone HSP70 (Minuzzo et al., 2000) as well as several cell cycle regulators such as the Sp1-regulated *p21* gene (Friedman et al., 2002). It is currently unknown whether Zalypsis affects RNA synthesis.

To gain further insight into the mechanism of action of these two antitumor tetrahydroisoquinolines, we investigated their

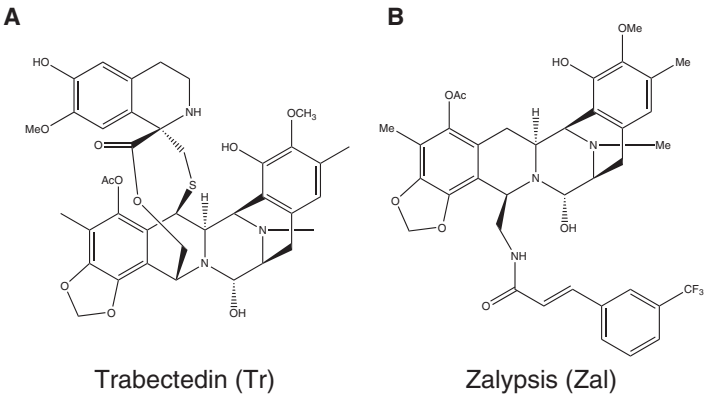

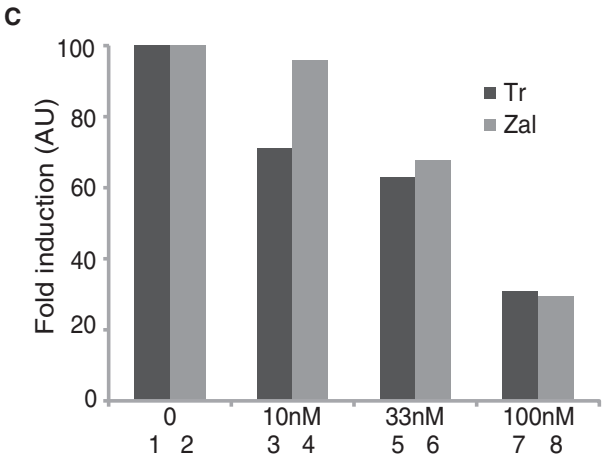

Figure 1. Cytotoxic Effects of Trabectedin and Zalypsis

Structures of trabectedin (A) and Zalypsis (B).

(C) Real-time PCR analysis of *RARβ2* induction by t-RA from HeLa cells pretreated with different concentrations of trabectedin (dark gray) and Zalypsis (light gray). The fold activation (noninduced versus induced) is shown, and *RARβ2* mRNA was normalized to *GAPDH* mRNA levels.

effect on transcription and DNA repair both in vitro and in vivo. By using a bead-immobilized SV40 promoter-containing DNA template, we explored whether trabectedin can compete with the transcription factor Sp1 for binding to its responsive elements and, therefore, prevent the accurate positioning of the transcription machinery around the promoter. We next assessed, by means of another bead-immobilized tailor-made oligonucleotide containing a single CGG triplet (a favored site for trabectedin and Zalypsis covalent bond formation) (Pommier et al., 1996), whether these drugs can inhibit RNA synthesis by preventing the formation of the preinitiation transcription complex and/or by blocking RNA polymerase II (RNA pol II) elongation (independently of the strand to which the drug is bonded), and we sought confirmation in HeLa cells. We also tested whether adducts formed by these drugs can be recognized by defined components of the NER machinery. Finally, computer modeling and molecular dynamics (MD) simulations help us to rationalize our experimental observations.

RESULTS

Antitumor Activities and Effects on Gene Expression of Trabectedin and Zalypsis

The growth inhibitory activity of the two drugs was evaluated in a panel of sarcoma (SW872, A673, and Saos-2), breast (MCF7), and ovarian (A2780) cancer cell lines. All the cancer cell lines tested were very sensitive to trabectedin and Zalypsis (Table 1), with IC_{50} values in the high picomolar/low nanomolar range (0.1–3.0 and 0.4–1.8 nM, respectively). Their effect on gene expression was studied in HeLa cells by monitoring transcription of the *RARβ2* gene, a retinoic acid-responsive gene whose expression was induced with 10^{-5} M all-trans retinoic acid (t-RA). We observed that 1 hr of exposure to increasing concentrations of trabectedin and Zalypsis before incubation with t-RA over 6 hr led to a dose-dependent inhibition of *RARβ2* gene expression. At 100 nM, 70% of *RARβ2* transcription was inhibited (Figure 1C).

Trabectedin Competes with the DNA-Binding Transcription Factor Sp1

DNA-binding transcription factors convey information by associating to their responsive elements. Thus, we investigated how these drugs could affect the binding of Sp1 (Dynan and Tjian, 1983), a ubiquitous transcription factor that specifically recognizes GC-rich sequences in many gene promoters. The Sp1-responsive element-containing SV40 promoter (Mathis and Chambon, 1981) was ^{32}P labeled, immobilized on magnetic beads, and incubated with increasing amounts of either Sp1-containing HeLa nuclear extracts (NEs) or trabectedin for 30 min before being washed to remove any nonspecific DNA-binding molecules. DNase I footprinting showed that increasing amounts of Sp1 protected the SV40 promoter between −106 and −45 as well as a stretch closer to the transcription start site, as visualized by the disappearance of the G_{-9} and C_{-10} hypersensitive sites (HSs) (Figure 2A, lanes 1–4). Trabectedin, which is known to possess high affinity for several GC-rich triplets (Pommier et al., 1996), also targets the Sp1-binding sites on the SV40 promoter in a dose-dependent manner, in addition to DNA sequences located at positions C_{-116} or C_{-119} and G_{-3} or G_{-7}, with a DNase I HS being visible at position G_{-60} (lanes 5–8).

Table 1. Growth Inhibitory Activities of Trabectedin and Zalypsis on Different Cancer Cell Lines

		IC_{50} (nM)[a]	
Tissue Type	Cell Line	Trabectedin	Zalypsis
Liposarcoma	SW872	0.5	0.8
Ewing sarcoma	A673	1.0	0.4
Osteosarcoma	Saos-2	0.1	0.9
Breast cancer	MCF7	2.6	1.8
Ovarian cancer	A2780	3.1	1.1

Tumor cells were seeded in 96-well trays and incubated with serial dilutions of each drug for 72 hr.

[a] Half-maximal inhibitory concentration.

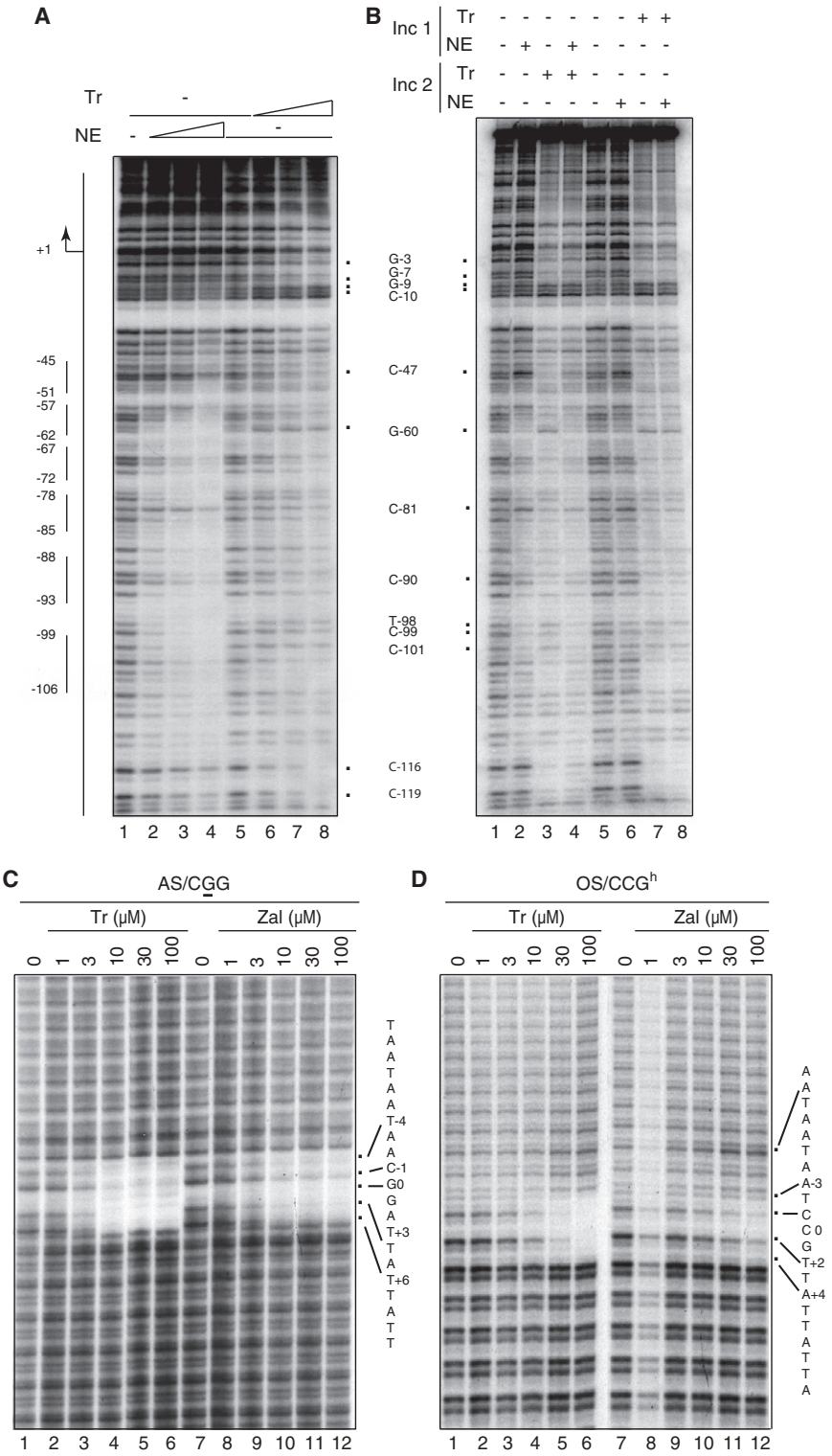

Figure 2. DNase I Footprinting Assays on the SV40 Promoter and on DNA Templates Containing a Unique Drug-Binding Site

(A) The ^{32}P-labeled and immobilized SV40 promoter was incubated with increasing amounts of either HeLa NE or trabectedin before being digested by DNase I. The Sp1-binding sites are shown at the right of the gel.

(B) Different rounds of incubation of either HeLa NE or trabectedin, as indicated at the top of the panel, were performed on the bead-immobilized SV40 promoter-containing DNA followed by DNase I treatment.

The AS/CGG (C) or OS/CCG^h (D) was incubated with increasing drug concentrations and treated with DNase I. The positions of the HS (A and B) or the protected nucleotides (C and D) are indicated (nb: for C and D the G0 is the guanine that is covalently bonded to the drug).

See also Figure S1.

To further investigate whether the DNA-binding factor and the drug compete for similar target sites, we set up a challenge assay based on sequential rounds of incubation of either Sp1 or trabectedin. When the DNA template was first incubated with Sp1-containing HeLa NE and then with the drug, we observed an extended protection originated by Sp1 itself (Figure 2B, lanes 4 and 2) and the absence of the drug-specific HS located at positions G_{-60}, T_{-98}, C_{-99}, and C_{-101} (compare lanes 4 and 3). This suggests that the drug does not displace Sp1 from its binding sites on the DNA template. The converse experiments, in which the DNA template was first incubated with the drug and then with Sp1, showed the same footprinting pattern as when the template was incubated with trabectedin alone (lanes 7 and 8). Thus, under the conditions employed, trabectedin competes with the transcription factor Sp1 for targeting specific DNA sequences (see Figure S1 available online).

Trabectedin and Zalypsis Protect from DNase I Digestion and Inhibit RNA pol II Transcription

To learn more about how these anticancer drugs affect RNA synthesis, we designed a bead-immobilized ^{32}P-labeled DNA substrate (Riedl et al., 2003) containing a unique, high-affinity, adduct-forming site (5′-CGG-3′) in just one strand flanked by TAA and ATT repeats on each side. After 30 min of exposure to increasing drug concentrations to saturate the high-affinity site, followed by extensive washing to remove any unbound molecules, this substrate was treated with DNase I. The AS/CGG was protected from DNase I digestion from nucleotides (nt) T_{-4} to T_{+6}, being G_0 the guanine to which trabectedin is covalently bonded (Figure 2C, lanes 1–6). The Zalypsis adduct led to a similar but weaker protection (lanes 7–12). An

identical concentration-dependent protection of the OS/CCG^h, which associates with either trabectedin or Zalypsis only through hydrogen bonds and van der Waals interactions involving the CCG^h triplet, was likewise detected from nt A_{-3} to A_{+4} (Figure 2D). These data show that the presence of the covalently bonded drugs in the minor groove of the DNA double helix specifically protects a CGG triplet and the surrounding nucleotides from DNase I access to both DNA strands. The use of 3- and 10-fold excesses of drug allowed us to confirm that this was a unique drug-binding site on the whole polynucleotide chain because no other footprints were apparent at these very high concentrations.

The effect of these drugs on RNA synthesis was investigated by performing an in vitro transcription assay using as template a 5′ end bead-immobilized DNA molecule containing the adenovirus major late promoter (AdMLP) in front of a G-less cassette (Figure 3A). Following preincubation with the indicated drug concentrations and washes to remove the excess of unbound drug, the beads were incubated with highly purified RNA pol II and the basal transcription factors TBP, TFIIB, TFIIE, TFIIF, and TFIIH, together with nucleotide triphosphates (NTPs) with the exception of GTP. Drug exposure resulted in decreased synthesis of RNA transcripts compared to controls (Figure 3B). In these experimental conditions we did not observe the presence of any shorter RNA transcripts due to premature RNA synthesis arrest (data not shown). Of note, Zalypsis completely inhibited transcription at a concentration of 1 μM (lane 10), whereas a much higher concentration of trabectedin was necessary to abolish transcription entirely (lane 4). This may indicate that Zalypsis is more potent than trabectedin in inhibiting RNA synthesis. Altogether, the above experiments suggest that some drug molecules target the promoter and thereby prevent formation of the transcriptional preinitiation complex, thus inhibiting RNA synthesis.

To assay the effects of trabectedin and Zalypsis on transcription elongation, we used another 5′ end bead-immobilized substrate containing, in addition to the AdMLP and the G-less cassette of 96 nt, a 127 nt long DNA sequence encompassing a CGG triplet at position +113 surrounded by AAT or ATT repeats (Figure 3A). The CGG drug-binding site was placed either on the transcribed strand (TS) or the nontranscribed strand (NTS). By following this strategy one trabectedin or Zalypsis adduct was placed on either the TS or the NTS DNA strand during RNA pol II elongation. The CGG/TS template was first incubated with all transcription components in the absence of GTP. In these conditions RNA pol II paused at the end of the G-less cassette (+96/+99). After several washes to remove both the remaining preinitiation complexes and the nonspecifically bound factors, the immobilized template containing only the elongating RNA pol II (Riedl et al., 2003; Zawel et al., 1995) was incubated with increasing drug concentrations. After washing off the excess of drugs, addition of all NTPs including GTP allowed RNA pol II to further elongate. We observed that both drugs inhibited full-length transcription (FLT: +223; Figure 3C, lanes 1–6 and 8–13, respectively). Zalypsis-dependent FLT inhibition was complete at a much lower concentration than that required by trabectedin (lanes 11–12 and 4–5). Furthermore, RNA pol II was blocked by trabectedin a few nucleotides before the CGG site targeted by the drug, i.e., at positions +108, +109, and +110 (lane 6), whereas Zalypsis arrested RNA pol II at +108 and +109 (lane 13). Another difference was the detection of a Zalypsis-specific RNA pol II stop site at position +98 (lane 13). This could be rationalized because this drug, but not trabectedin, binds to the 5′-TGT-3′ triplet and stabilizes a duplex containing this sequence (Leal et al., 2009).

Strikingly, when we investigated whether RNA pol II elongation could also be affected by the presence of a trabectedin or Zalypsis adduct in the CGG/NTS, FLT inhibition was observed not only at the same drug concentrations but also at the same nucleotide positions that were identified previously on the CGG/TS construct (Figures 3C and 3D, compare lanes 5 and 11). This result strongly supports the view that the adducts formed by either trabectedin or Zalypsis mimic ICLs.

Trabectedin and Zalypsis Promote the 5′ XPF/ERCC1-Dependent Incision

We next investigated whether the binding of trabectedin and Zalypsis to DNA would interfere with NER, given the established connection between these drugs and several NER factors (Takebayashi et al., 2001). To examine whether the NER machinery could eliminate this type of DNA damage, we incubated internally labeled polynucleotides containing a single drug-binding site with the drugs. After extensive washing, we added the highly purified NER factors XPC/HR23B, TFIIH, XPA, RPA, XPG, and XPF/ERCC1 (hereafter XPF) and ATP. In these conditions we did not observe removal of the damaged oligonucleotide (data not shown), but rather unexpectedly, we detected that the OS/CCG^h strand was cut at positions A_{-4} and A_{-3}, whereas the AS/CGG strand (drug adduct at the underlined guanine) was slightly incised at positions T_{-7} and A_{-5} (Figure 4A, lanes 2 and 6). XPF endonuclease was responsible for this cleavage because the incision signal was lost in its absence (lane 7), whereas the OS/CCG^h substrate was still cleaved when XPG was omitted (lane 8). Furthermore, the OS/CCG^h pretreated with either trabectedin (Figure 4C) or Zalypsis (Figure 4E) was better cut by XPF in a concentration-dependent manner, but the AS/CGG template was not significantly cleaved (Figures 4B and 4D).

We reasoned that the weak XPG-uncoupled XPF-dependent cut on the drug-free DNA template (Figures 4B and 4D, lanes 1–5) must be due to the particular choice of TAA and ATT repeats on each side of the CGG target triplet giving rise to a sequence-dependent deformation of the DNA helix (most likely melting) that is partially recognized by XPF. This interpretation was supported by results from MD simulations of a solvated 15-mer in 0.1 M NaCl at 400 K, i.e., under conditions that favor strand separation. Indeed, initial fraying of the oligomer's ends was followed by splaying and complete melting of the two strands after ~200 ns, whereas the base pairs making up the central CGG triplet in the drug-modified DNAs remained hydrogen bonded throughout the whole simulation (Figure S2; unpublished data).

We also found that in the presence of replication protein A (RPA), which plays a role in all DNA metabolic processes involving ssDNA, the XPF-dependent incision on the OS/CCG^h — that is enhanced by trabectedin — was stimulated still further (Figure 4F, lanes 15–18). Remarkably, the weak XPF-dependent cuts observed in the absence of drug on the AS/CGG template at positions T_{-7} and A_{-5} (lanes 5 and 9), and on

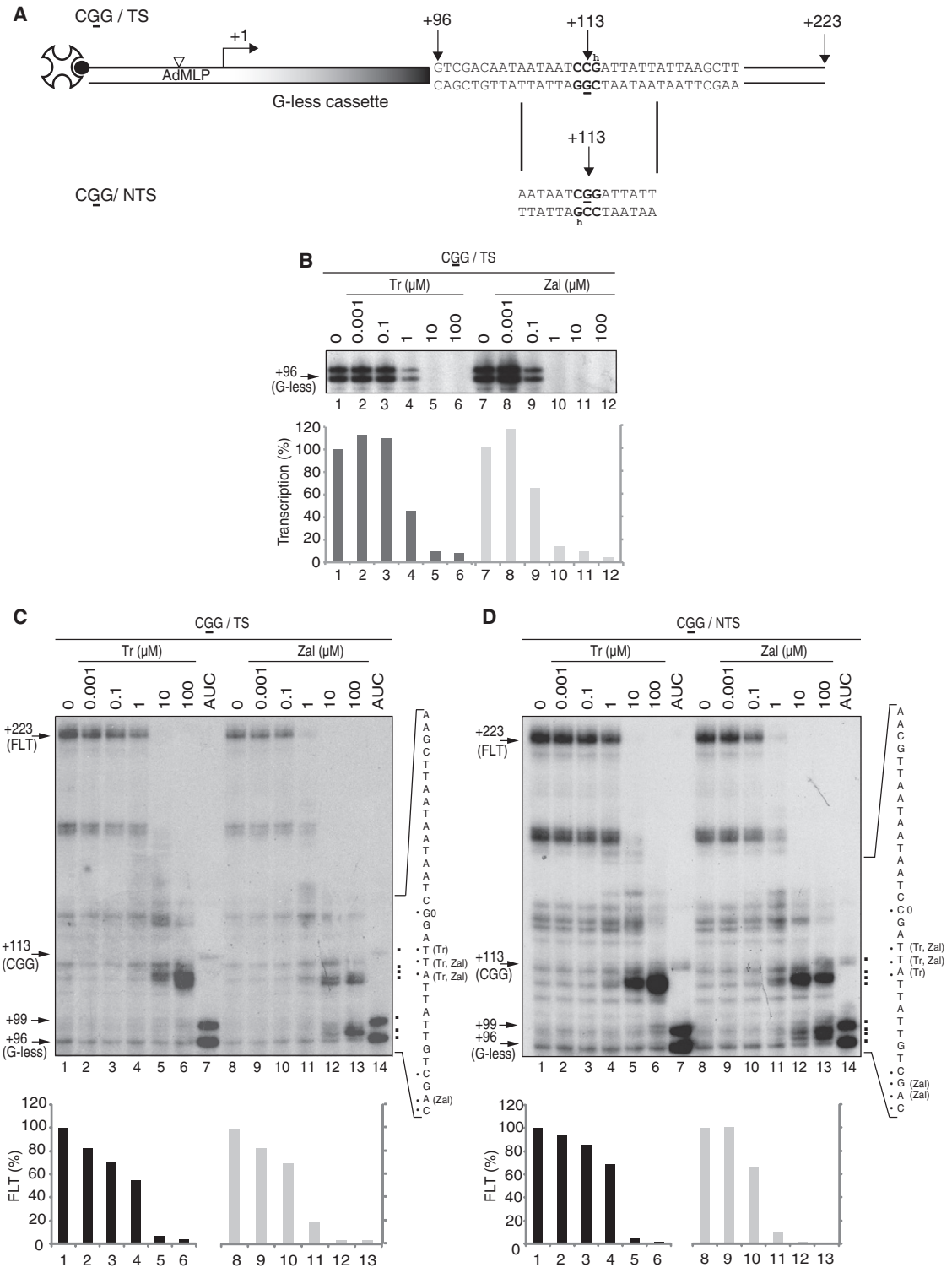

Figure 3. Effects of Trabectedin and Zalypsis on Transcription

(A) Scheme of the 5′ end-immobilized DNA containing the unique binding site 5′-CGG-3′. The drug-modified guanine (G) is positioned at +113 bp of the transcription start site (+1) either on the CGG/TS or the CGG/NTS.

(B) The DNA template was incubated with amounts of drug as indicated. Quantification of the +96 and +99 nt long transcripts was performed using the ImageJ software.

The CGG/TS (C) and the CGG/NTS (D) DNA templates were transcribed in the presence of NTPs except GTP, leading to RNA pol II arrest at the end of the G-less-cassette. After incubation with increasing amounts of trabectedin and Zalypsis and washing off the unbound drug, transcription was resumed in the presence of

the OS/CCG^h at position C_{-1} (lanes 15 and 17), became undetectable at high drug concentrations. This demonstrates how the drug-modified DNA becomes a suitable substrate for the XPF endonuclease. In the presence of Zalypsis, we also observed a dose-dependent stimulation of the OS/CCG^h cleavage (Figure 4F, lanes 20–23). However, the incision located at position A_{-3} on this strand predominated over that appearing at position A_{-4} (lanes 22–23) when compared to the results obtained in the presence of trabectedin (lane 17). Interestingly, in the case of Zalypsis, RPA partially inhibited the XPF-dependent incision on the OS/CCG^h strand. This illustrates that our system is able to translate the structural differences between the two drugs into macroscopic observables. Altogether, the above data show how trabectedin and Zalypsis promote the formation of a DNA structure that allows a specific 5′ XPF-dependent incision on the OS/CCG^h DNA, i.e., the strand opposite to that containing the drug adduct.

Trabectedin and Zalypsis Induce DNA Strand Breaks In Vivo

The trabectedin- and Zalypsis-dependent induction of DNA strand breaks was evaluated in HeLa cells using the comet assay, which is based on the alkaline lysis of labile DNA at sites of damage (Collins et al., 2008). DNA from cells that have accumulated damage appears as fluorescent comets with tails of DNA fragmentation or unwinding, whereas normal, undamaged DNA does not migrate far from the origin (Figure 5A). We next investigated how the silencing of XPF (using HeLa cells that stably express siRNA against XPF, HeLa siXPF) would affect the generation of DNA breaks. Both HeLa siCtrl and HeLa siXPF cells were treated with trabectedin and Zalypsis at 10 and 100 nM for 15 hr. We observed a clear concentration-dependent increase in DNA strand breaks in both cell lines following treatment with either drug (Figures 5B and 5C). Of note, HeLa siXPF cells showed a lower amount of DNA breaks after drug treatment compared to HeLa siCtrl cells. With trabectedin these differences were observed only at 100 nM ($p < 0.01$), whereas with Zalypsis, they were observed at the two drug concentrations tested (10 and 100 nM; $p < 0.01$). Notably, no major differences in formation of γ-H2AX foci, a DSB marker, were found upon drug treatment in siCtrl and siXPF cells (Figure S3), consistent with earlier reports for mitomycin C (Niedernhofer et al., 2004). Altogether, our results suggest that XPF endonuclease is involved in the formation of drug-induced single-strand DNA breaks (SSBs).

DISCUSSION

We and others showed that both trabectedin and Zalypsis inhibit the growth of a variety of cancer cell lines and tumor cells (D'Incalci and Jimeno, 2003; Leal et al., 2009; Ocio et al., 2009) (Table 1). However, the cell type-sensitivity pattern for trabectedin is different from that observed for Zalypsis because the former drug shows selectivity against sarcoma, breast, ovarian, and lung tumor cell lines, with head-and-neck and colon tumor cells being slightly less sensitive, whereas the latter is more potent against leukemia and stomach tumor cell lines, with breast cancer cells being slightly less sensitive than the average (Koeppel et al., 2004; Poindessous et al., 2003). The aim of the present work is to improve our understanding of the particular and specific mode of action of these drugs and highlight any differences between the two.

Trabectedin and Zalypsis Mimic "DNA Interstrand Crosslinkers"

The first step in the binding of a typical bifunctional agent to DNA is the formation of a monoadduct, and this is followed by a second reaction, on either the same strand (intrastrand) or the complementary strand (interstrand), leading to the formation of a crosslink (Muniandy et al., 2010). By covalently linking the two complementary strands of the double helix, ICLs prevent DNA melting, transcription, and replication: hence, they are considered as the most toxic lesions induced by chemotherapeutic agents (Ben-Yehoyada et al., 2009). Because the thermal stability of a DNA duplex increases substantially by the presence of a single bonded trabectedin or Zalypsis molecule (Casado et al., 2008; Leal et al., 2009), this type of monoadduct could represent the same complex challenge to DNA repair mechanisms, as does an ICL. Here, we produce additional evidence that the adducts formed by both trabectedin and Zalypsis functionally mimic a typical ICL despite the fact that these drugs bind covalently to only one DNA strand, their interaction with the OS being only through van der Waals contacts and hydrogen bonds. These ICL-mimetic properties were first illustrated by footprinting assays that demonstrated how the drugs specifically protect the high-affinity CGG sequence, as well as the complementary triplet in the OS, from DNase I digestion (Figure 2). The observed differences in the DNase I footprinting patterns, together with subtly distinct effects in the transcription and repair assays (Figures 3 and 4), reflect the structural variations in the drug substituent that protrudes out of the minor groove in the covalent complexes formed with dsDNA, i.e., a tetrahydroisoquinoline for trabectedin (García-Nieto et al., 2000) and a trifluorocinnamic moiety for Zalypsis (Leal et al., 2009). Because these drugs "interact," albeit in different ways, with both DNA strands, it is not surprising that NER was ineffective in removing the adducts (data not shown), contrary to what is seen with UV- or cisplatin-damaged DNA: neither XPC, XPE, nor XPA would recognize and unwind the damaged DNA (Aboussekhra et al., 1995). Likewise, XPC is inefficient in recognizing the highly tumorigenic benzo[a]pyrene diol epoxide DNA adducts that are known to weaken Watson-Crick hydrogen bonding and base-base stacking interactions and give rise to local thermal destabilization of the double helix (Schinecker et al., 2003).

Trabectedin and Zalypsis Promote DNA Cleavage by XPF

Further support for the ICL-mimetic properties of the drug-DNA adducts studied was obtained when we discovered the

all NTPs including GTP. The RNA transcripts were analyzed on a 5% denaturing urea gel, and quantifications of the full-length transcripts (FLT, +223 bp) were performed. Trabectedin or Zalypsis-mediated stops were detected close to the 5′-CGG-3′ containing region (+113 nt). The drug-induced RNA pol II arrests are indicated in brackets on the sequence on the right of each gel.

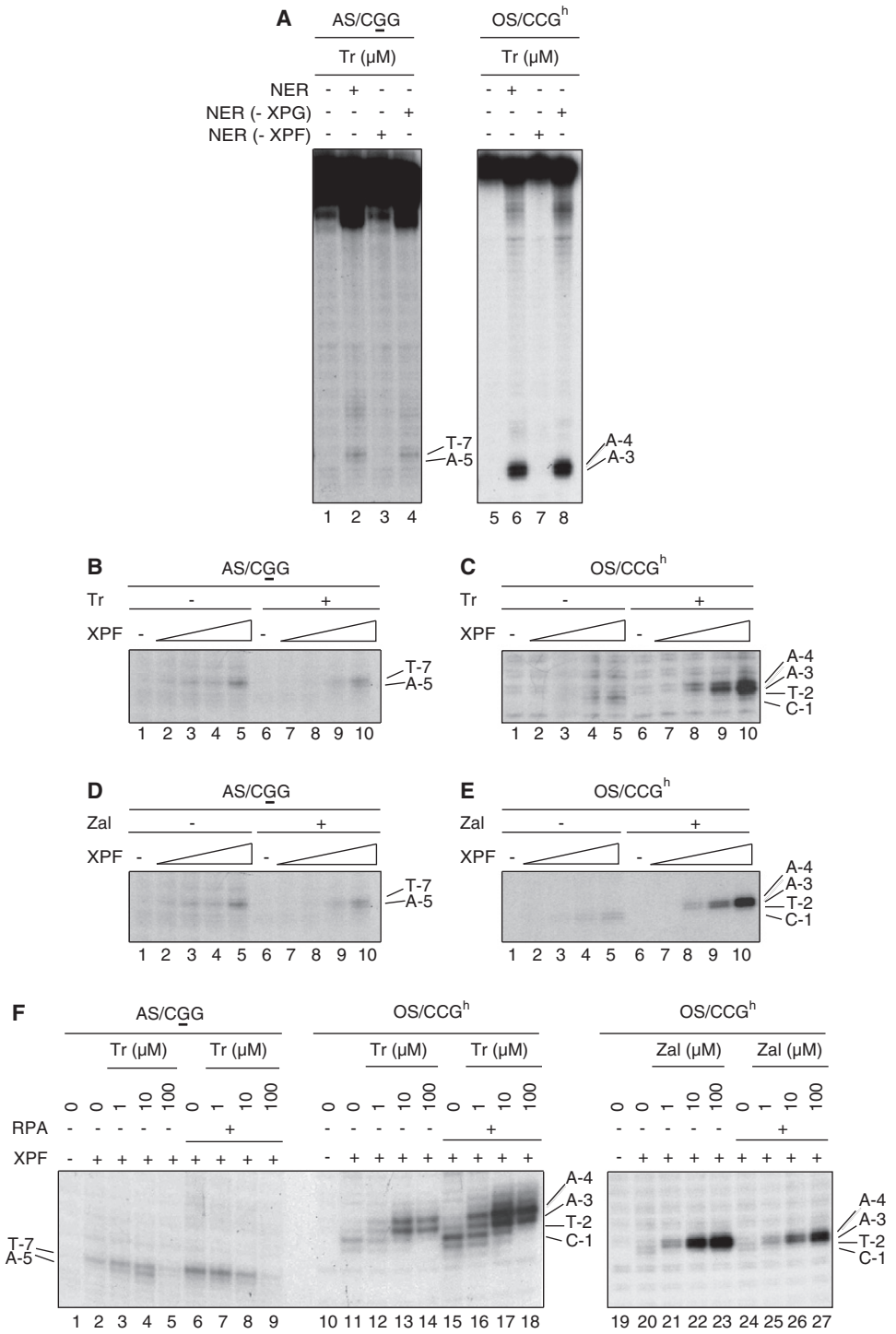

Figure 4. Trabectedin- and Zalypsis-Dependent Effects on DNA Incision

(A) Characterization of the incision on the AS/CGG and the OS/CCG^h pretreated with trabectedin and incubated with NER factors in the presence or absence of XPG and XPF.

XPF-dependent incision on either the AS/CGG or the OS/CCG^h in the presence or absence of either trabectedin (B and C) or Zalypsis (D and E). (F) RPA-mediated effect on the trabectedin (right panel)- and Zalypsis (left panel)-dependent incision using the AS/CGG and the OS/CCG^h substrates.

See also Figure S2.

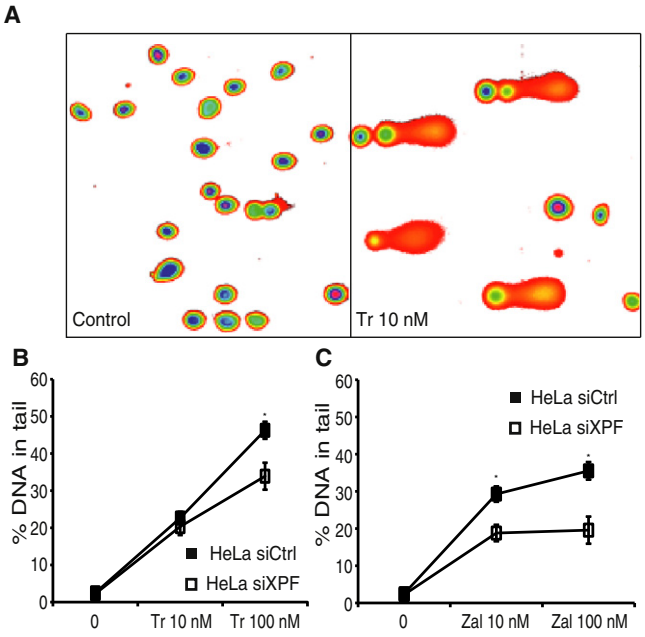

Figure 5. Trabectedin and Zalypsis Induce DNA Breaks In Vivo

(A) Representative images of damaged DNA in the comet assay in untreated and trabectedin-treated (for 12 hr) HeLa cells. HeLa siCtrl and HeLa siXPF cells were analyzed through comet assay followed by exposure to (B) trabectedin and (C) Zalypsis at 10 and 100 nM during 15 hr. Cells were treated, washed with PBS, detached mechanically, and included in low melting point agarose. After lysis, cells were subjected to electrophoresis, and the comets were stained with SYBR Green. DNA quantitation in the comets was performed with TriTek CometScore Freeware version 1.5 ($p < 0.001$). Pictures were taken with a Leica DM IRM fluorescence microscope equipped with a DFC 340 FX digital camera (Leica, Wetzlar, Germany). A minimum of 200 cells was analyzed, and the experiments were repeated in duplicate. The Mann-Whitney U test was used for the statistical analysis. See also Figures S3 and S4.

enhanced cutting of the DNA substrates containing trabectedin or Zalypsis by XPF, a structure-specific endonuclease that preferentially cleaves DNA duplexes adjacent to a 3′ ss flap (Mocquet et al., 2007) and that has been shown to recognize partially unwound structures near a psoralen-induced ICL (de Laat et al., 1998). Drug-induced DNA strand breaks in living cells were assessed by the comet assay and γ-H2AX staining (Figure 5; Figure S3). The finding that SSBs decreased following silencing of XPF expression strongly suggests that the drug-bonded DNA provides an accurate 3D substrate that is recognized and acted upon by the XPF endonuclease, a key player in multiple steps of ICL repair (Kuraoka et al., 2000; Soares et al., 2007).

The extreme sensitivity to trabectedin of HR-deficient cells, which is similar to that evoked by the minor groove-binding and ICL-forming mitomycin C (Rahn et al., 2010), is indeed suggestive that the type of monoadducts formed by these tetrahydroisoquinolines can functionally behave like an ICL. In fact when DNA strand separation is effectively prevented, replication and transcription forks stall, and this event is known to trigger the recruitment of XPF/ERCC1, together with RPA, for 5′ cleavage of the damaged DNA. Support for this interpretation was obtained from MD simulations results, which clearly showed that the melting of the target oligonucleotide at, and on both sides of, the central CGG triplet is hampered in the presence of the bonded drugs (Figure S2). These observations imply that trabectedin and Zalypsis contribute to extending the length of the Watson-Crick base-paired central region and, therefore, enhance XPF recognition and binding by stabilizing a ds/ss discontinuity and one or two 3′ DNA flaps.

To account for the positions of the incisions catalyzed by XPF when either trabectedin or Zalypsis is bonded to the CGG target site, we built molecular models of human XPF/ERCC1 in complex with 5′-$(TAA)_2$CGG$(ATT)_2$-3′. The DNA-binding domain (DBD) of ERCC1 recognizes dsDNA, and the nuclease domain of XPF cuts one strand of this dsDNA at the 5′ side of a junction with ssDNA. The exact cleavage position varies from 2 to 8 nt away from the junction (Mu et al., 2000), and it appears that the ssDNA arm protruding in the 3′ direction (the "3′-flap" or "3′-overhang") is the only requisite for the positioning of the incisions carried out by XPF/ERCC1. Our modeled structures indicate that two different cleavable complexes need to be formed to account for the cuts on either the AS/CGG or OS/CCG^h of the DNA molecule, but the observation of an incision only at the OS/CCG^h indicates that only one is feasible in the presence of the drugs (Figure 4). We note that to cleave the AS/CGG, the required ssDNA region favored by the TA surroundings could start forming at the first A located 3′ to the central CGG dsDNA stretch. However, the presence of a drug molecule covalently bonded to the middle (underlined) guanine in this triplet hampers DNA melting and, hence, cutting of this strand by the nuclease, which cannot find the mandatory 3′ flap. On the contrary, the ssDNA region in the OS can start forming following the T placed 3′ to the CCG^h triplet, whereas the dsDNA stretch will comprise the central CGG/CCG^h plus a variable number of paired bases 5′ to the first C (in CCG^h) that is longer for the trabectedin adduct, and shorter for the Zalypsis adduct (Figures 6A and 6B). Of note, the structural differences between the two drugs studied here are also found in this region, with trabectedin establishing an additional H bond between the phenolic oxygen in the protruding tetrahydroisoquinoline and the phosphodiester backbone (García-Nieto et al., 2000) and Zalypsis sticking out a trifluorocinnamic moiety into the solvent/protein environment.

Although the comet assay showed that the SSBs depended on XPF (Figure 5), the silencing of individual NER factors (XPG or XPF/ERCC1) rendered the cells neither resistant nor hypersensitive to these drugs (Figure S4). These observations suggest that inducing the XPF-dependent DNA cuts is not the main cytotoxic mechanism harnessed by these drugs and that their activity should follow an alternative pathway.

Trabectedin and Zalypsis Inhibit RNA pol II Transcription

Finally, extra support for the ICL-mimetic hypothesis was gained when we showed that DNA damage caused by both drugs obstructs the expression of activated genes (Figure 1). The binding of these drugs to particular sequence triplets, located within certain responsive elements of the promoter of a given gene, might prevent the formation of the transcription complex. This was documented by challenge experiments between trabectedin and the transcription factor Sp1 competing to bind to GC-rich sites (Figure 2; Figure S1). Our results additionally

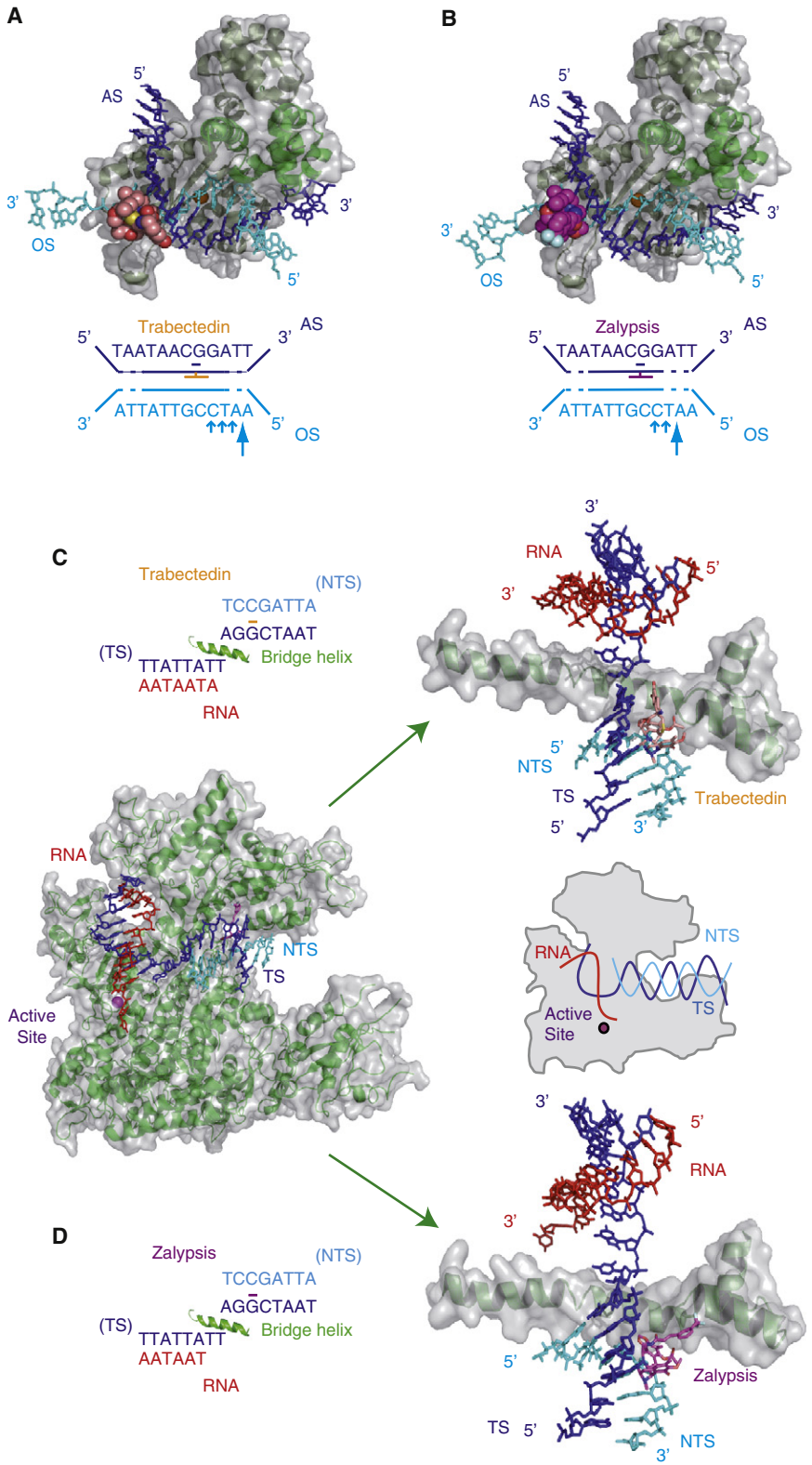

Figure 6. Impact of Trabectedin and Zalypsis on DNA Incision and Transcription Processes

Trabectedin (A) and Zalypsis (B) stimulate an XPF-dependent incision on the OS/CCG^h, i.e., the strand opposite to that harboring the drug adducts. Trabectedin (C) and Zalypsis (D) block RNA pol II progression when the drug is located either on the TS or the NTS. Only the complex structure containing the longest possible RNA transcript is represented for each drug. The schematic representation of RNA pol II is based on Figure 4 from Cramer (2004).

demonstrate that trabectedin and Zalypsis cause RNA pol II stalling regardless of whether the covalent adduct is present on the TS or the NTS (Figure 3). Such property supports the ICL-mimetic behavior of the drug-DNA adducts, which likely underlies the potent cytotoxicity of these compounds, and is in stark contrast with observations made for other adducts (de Laat et al., 1998), which do not have such an effect on transcription elongation when placed on the NTS. It must be kept in mind that the foremost DNA adduct for cisplatin is the 1,2-GG intrastrand crosslink and that less than 8% of cisplatin lesions consist of ICL (Frit et al., 2002; Schinecker et al., 2003). Therefore, the major difference between these two types of adducts is that the key lesion involving cisplatin affects the major groove of two contiguous guanines in the same strand, whereas in the case of the minor groove-binding tetrahydroisoquinolines studied here, the presence of the covalently bonded drug affects both strands and stabilizes the duplex structure. As a consequence, DNA strand separation is hampered regardless of which strand bears the lesion, and RNA pol II is arrested during transcription elongation. This finding could be relevant to the mechanism of cytotoxicity exerted by these drugs.

From the structural point of view, we provide an explanation in atomic detail for the differential arrest of RNA pol II synthesis (Figures 6C and 6D) in light of available crystal structures of RNA pol II elongation complexes (Huang et al., 1995; Stehlikova et al., 2002). Indeed, the number of base pairs between the drug adducts and the ssDNA-RNA hybrid past the polymerase active site was found to be slightly different in the modeled complexes involving each separate drug and to be in good accordance with the distinct sizes obtained for the RNA transcripts. Thus, three alternative models for the trabectedin-DNA-RNA pol II complex are possible,

depending on the relative location of the covalently modified guanine with respect to the active site, but only two in the case of Zalypsis due to the extended protrusion of the trifluorocinnamic moiety giving rise to steric clashes with the protein and precluding further movement of RNA pol II along the DNA template. For simplicity we present only one structure of the putative complex containing the DNA-bonded drug and the longest possible RNA transcript (Figures 6C and 6D). Because translocation over the bridge helix is prevented due to the presence of the drug on either strand, completion of the next nucleotide addition cycle is not feasible, and the RNA transcript is prematurely terminated.

In conclusion our study shows that the anticancer compounds trabectedin and Zalypsis, upon binding to DNA, give rise to a lesion that functionally mimics an ICL even though these drugs are covalently linked to only one DNA strand. These drugs promote XPF/ERCC1-dependent DNA breaks, inhibit RNA synthesis regardless of which DNA strand contains the adduct, and may prevent binding of Sp1, as shown here, and/or other transcription factors. However, it still remains to be seen whether these ICL-mimicking adducts can also preclude or stimulate the recruitment of one or more of the HR proteins that are likely to participate in the removal of these covalent modifications from damaged DNA.

SIGNIFICANCE

Exposure of cells to trabectedin or Zalypsis eventually gives rise to DNA double-strand breaks that do not originate directly from drug binding to the amino group of selected guanines in the minor groove of DNA but are formed during the processing of the resulting covalent adducts by the DNA repair machinery. Intriguingly, cells defective in homologous recombination (HR) repair are particularly sensitive to these agents, whereas cells deficient in nucleotide excision repair (NER) are more resistant to trabectedin than their NER-proficient counterparts. Using well-defined in vitro and in vivo assays, we now show that the DNA adducts formed by these two potent anticancer agents are not removed by the NER machinery, although the XPF/ERCC1 nuclease is able to cleave the strand opposite the lesion in a drug-dependent way. Furthermore, these adducts compete with DNA-binding factors like Sp1 for their specific DNA-binding sites and also arrest elongating RNA polymerase II at the site of the lesion regardless of whether the compounds are covalently attached to the template or the nontemplate strand. All of these results, which are supported by structural models, are consistent with the view that a single adduct formed by any of these drugs in just one DNA strand can functionally mimic an interstrand crosslink insofar as it can hamper or prevent repair and strand separation very effectively. Therefore, it would seem that stalling transcription and replication forks is likely to be a hallmark of the antiproliferative action of these tetrahydroisoquinoline alkaloids. Moreover, identification of the genes involved in their mechanism of action, and particularly in the DNA damage response, that are deregulated in a given tumor may help to select the subsets of patients that will benefit the most from this type of chemotherapeutic agent.

EXPERIMENTAL PROCEDURES

Activated Transcription

HeLa cells were grown to 50% confluency before being subjected to media containing charcoal-treated FCS (10%) and devoid of phenol red for 16 hr. Then, cells were pretreated for 1 hr with either drug, before t-RA induction (10 μM for 6 hr). Reverse transcription was done using 1 μg of total RNA (GenElute Mammalian Total RNA Miniprep Kit; Sigma-Aldrich), oligo-$dT_{(15)}$, and SuperScript II Reverse Transcriptase (Invitrogen).

Design of the DNA Templates

The SV40 promoter was PCR amplified from pGL3 vector (Promega) using a 5′ radioactively labeled primer with Optikinase (USB Corp.) and 100 nM γ^{32}P-dATP (6000 Ci/mmol), a biotinylated primer, and resolved on a 5% native 1× TBE polyacrylamide (PAA) gel. The DNA substrates containing a single CGG site for drug binding were generated by heating the forward ($A[TAA]_{20}$**CGG**ATTATT) and the reverse ($AA[TAA]_{20}$**CCG**TTATT) primers at 95°C for 5 min and slowly cooling down to 4°C. The Klenow fragment was used for fill-in synthesis during 30 min at 25°C in the presence of 1 mM dNTPs. The purified amplicon (QIAGEN PCR) was cloned into pGEM-T plasmid (Invitrogen) leading to pGEM-T 1xCGG containing the following sequence: $AT(TAA)_{13}$**CGG**$(ATT)_{19}$T. The AS/CGG and the OS/CCG^h-labeled templates were generated by digesting 100 μg pGEM-T 1xCGG using SpeI for AS/CGG, and NcoI for OS/CCG^h (50 U for 3 hr). Biotinylated and radioactive nucleotides were filled in using 30 U Klenow fragment, 50 μM dATP/dGTP, 20 μM Biotin-16-dUTP (Roche Diagnostics), and 130 nM α^{32}P-dCTP (3000 Ci/mmol) (GE Healthcare) at 37°C, followed by a second enzyme digestion (NcoI for AS/CGG and SpeI for OS/CCG^h) overnight at 37°C. The probe was resolved on an 8% native PAA gel.

The pBL-CAX TS.500 (Charlet-Berguerand et al., 2006) was digested by XbaI and SalI. A G-less cassette was PCR amplified (Sawadogo and Roeder, 1985) using High Fidelity polymerase (Roche), the XbaI-restriction site containing specific primers, and then digested by XbaI and SalI, gel purified, and ligated using NEB's Quick Ligation Kit protocol. The remaining G in the XbaI restriction site was changed to a C by performing site-directed mutagenesis using Phusion polymerase (Finnzymes) and specific primers. After gel purification, the PCR amplicon was ligated using T4 ligase (NEB) leading to the pBL-Gless96-CAX TS.500.

To insert the single drug-binding site into the pBL-G-less96-CAX TS.500, we deleted the sequence located after the G-less cassette using primers with the QuikChange Site-Directed Mutagenesis Kit (Stratagene). Then, we inserted the single drug-binding triplet into the plasmid using primers leading to the pBL-Gless96-CAX TS.500 CGG/TS and pBL-Gless96-CAX TS.500 CGG/NTS.

DNase I Footprinting Assays

The 5′ end ^{32}P-labeled (20,000 cpm) SV40 promoter template was immobilized on 2.01 × 10^5 magnetic beads (Dynabeads), incubated for 30 min at RT in buffer A (Tris/HCl 10 mM [pH 7.6], glycerol 10%, EDTA 1 mM, DTT 0.5 mM, KCl 50 mM, and 0.05% NP40), and then incubated either with 1–5 μg/μl of HeLa Sp1 containing NE or with 10–20 μM trabectedin for 30 min. For the competition assay the above substrate was incubated first with either 3 μg/μl of NE or 20 μM trabectedin for 30 min, and vice versa in a second incubation. Low-salt concentration washes were then performed to remove any DNA-unbound molecules before subjecting the DNA template to digestion using 1 ng/μl DNase I (Sigma-Aldrich) for 45 s at RT in buffer A supplemented with 5 mM $MgCl_2$, and 20 μg/ml polydI-dC.

The 3′ end-labeled (20,000 cpm) pGEM-T 1xCGG-derived AS/CGG or the OS/CCG^h substrates were bound to magnetic beads and treated with the indicated drug concentrations. Unspecific bound molecules were removed by gently washing with buffer A before DNase I digestions. The reaction was stopped, and the purified nucleic acids were resolved on an 8% denaturing urea-PAA gel.

In Vitro Transcription

The immobilized pBL-Gless96-CAX TS.500 CGG/TS or the pBL-Gless96-CAX TS.500 CGG/NTS PCR-amplified product was incubated with the drug. After extensive washing, the template was incubated with all the basal transcription factors including RNA pol II for 30 min at 25°C (Charlet-Berguerand et al.,

2006); then 300 μM ATP/UTP, 10 μM cold CTP, and 5 μCi α-^{32}P-CTP (3000 Ci/mmol) were added for 30 min at 25°C.

For the investigation of the drugs' effects on transcription elongation, the template was first incubated with all the basal transcription factors and rNTPs except GTP. After extensive washes (Riedl et al., 2003), the ternary elongation complex was incubated for 30 min with the drug in buffer A containing rNTPs (in the absence of GTP). After washes with buffer A, 300 μM rNTPs and 6.5 mM $MgCl_2$ were added. Nucleic acids were analyzed on a 5% denaturing urea-PAA gel.

Comet Assay

For the comet assay a single-cell gel electrophoresis assay was used (Trevigen's CometAssay) following the manufacturer's instructions after treatment of cells for 12 hr with the appropriate concentration of trabectedin and Zalypsis. Pictures were taken with a Leica DM IRM fluorescence microscope equipped with a DFC 340 FX digital camera (Leica, Wetzlar, Germany). Quantitation of the DNA in the tails of the comets was performed with Adobe Photoshop CS3 (Adobe Systems Inc., San Jose, CA). For each condition 30 cells were analyzed, and the experiments were repeated several times.

Molecular Modeling

XPF/ERCC1 in Complex with Drug-Bound DNA

The nuclease domain of human XPF was modeled using the coordinates of *Pyrococcus furiosus* Hef as a template (PDB ID: 1J23) and the sequence alignment (Kelley and Sternberg, 2009). The resulting structure and the DBDs of XPF and ERCC1 (PDB ID: 2A1J) were superimposed onto their DBD counterparts in the *Aeropyrum pernix* XPF homodimer in complex with dsDNA (PDB ID: 2BGW). The root-mean-square deviation between the Cα traces of human and crenarchaeal XPF nuclease domain was 1.1 Å, whereas that between their DBDs was 1.26 Å (53 atoms). The *A. pernix* XPF-dsDNA structure comprises two XPF protomers and one DNA duplex, bound to the nuclease and $(HhH)_2$ domains of the first protomer (site I). Because the $(HhH)_2$ domain of the second protomer (which corresponds to ERCC1) is also potentially capable of binding DNA (site II), a second dsDNA molecule was built at 90° to the experimentally observed dsDNA using a symmetry operator on the DNA in the unit cell as reported in Newman et al. (2005). The DNA-drug adducts were modeled as reported for trabectedin in PDB/OCA entry 1EZH (García-Nieto et al., 2000).

Drug-DNA-RNA Pol II Elongation Complex

The crystal structure of the RNA pol II elongation complex (Sydow et al., 2009), containing both a DNA template and an RNA transcript (PDB ID: 3HOV), was used upon appropriate substitution of DNA bases so as to model the oligonucleotide employed in our experiments. The position of the CGG triplet to which trabectedin and Zalypsis bind in relation to the polymerase active site was systematically varied stepwise to define those locations in which the drug would give rise to steric clashes with the protein. All primer sequences are available upon request.

SUPPLEMENTAL INFORMATION

Supplemental Information includes four figures and can be found with this article online at doi:10.1016/j.chembiol.2011.06.007.

ACKNOWLEDGMENTS

We dedicate this work to our collaborator Jonathan Gintz. We also acknowledge Professor J.M. Fernández-Sousa, Dr. Carmen Cuevas, and Dr. Frédéric Coin for fruitful discussions. We are grateful to C. Braun, A. Larnicol, B. Prève, and G. Santamaria Nunez for purification of repair and transcription factors and cell toxicity assays. We want also to thank Denis Biard for the HeLa siXPF. This work was supported by l'Association de la Recherche contre le Cancer (ARC n°3153), la Ligue contre le Cancer, INCA, and an ERC Advanced grant (to J.M.E.), and Comisión Interministerial de Ciencia y Tecnología (SAF2006-12713-C02-02 and SAF2009-13914-C02-02) and Comunidad de Madrid (S-BIO/0214/2006) (to F.G.). S.F. was supported by an ARC and Marie Curie fellowship, and C.G. is a recipient of a fellowship from the Ministère de la Recherche and ARC. M.M.-D. is an employee of PharmaMar, and C.M.G. is an employee and shareholder of Pharma Mar.

Received: March 12, 2011
Revised: June 3, 2011
Accepted: June 17, 2011
Published: August 25, 2011

REFERENCES

Aboussekhra, A., Biggerstaff, M., Shivji, M.K., Vilpo, J.A., Moncollin, V., Podust, V.N., Protić, M., Hübscher, U., Egly, J.M., and Wood, R.D. (1995). Mammalian DNA nucleotide excision repair reconstituted with purified protein components. Cell *80*, 859–868.

Ben-Yehoyada, M., Wang, L.C., Kozekov, I.D., Rizzo, C.J., Gottesman, M.E., and Gautier, J. (2009). Checkpoint signaling from a single DNA interstrand crosslink. Mol. Cell *35*, 704–715.

Bustamante, C., Cheng, W., and Mejia, Y.X. (2011). Revisiting the central dogma one molecule at a time. Cell *144*, 480–497. Erratum: (2011). Cell *145*, 160.

Casado, J.A., Río, P., Marco, E., García-Hernández, V., Domingo, A., Pérez, L., Tercero, J.C., Vaquero, J.J., Albella, B., Gago, F., and Bueren, J.A. (2008). Relevance of the Fanconi anemia pathway in the response of human cells to trabectedin. Mol. Cancer Ther. *7*, 1309–1318.

Charlet-Berguerand, N., Feuerhahn, S., Kong, S.E., Ziserman, H., Conaway, J.W., Conaway, R., and Egly, J.M. (2006). RNA polymerase II bypass of oxidative DNA damage is regulated by transcription elongation factors. EMBO J. *25*, 5481–5491.

Collins, A.R., Oscoz, A.A., Brunborg, G., Gaivão, I., Giovannelli, L., Kruszewski, M., Smith, C.C., and Stetina, R. (2008). The comet assay: topical issues. Mutagenesis *23*, 143–151.

Cramer, P. (2004). RNA polymerase II structure: from core to functional complexes. Curr. Opin. Genet. Dev. *14*, 218–226.

Cuevas, C., and Francesch, A. (2009). Development of Yondelis (trabectedin, ET-743). A semisynthetic process solves the supply problem. Nat. Prod. Rep. *26*, 322–337.

Damia, G., Silvestri, S., Carrassa, L., Filiberti, L., Faircloth, G.T., Liberi, G., Foiani, M., and D'Incalci, M. (2001). Unique pattern of ET-743 activity in different cellular systems with defined deficiencies in DNA-repair pathways. Int. J. Cancer *92*, 583–588.

de Laat, W.L., Appeldoorn, E., Jaspers, N.G.J., and Hoeijmakers, J.H.J. (1998). DNA structural elements required for ERCC1-XPF endonuclease activity. J. Biol. Chem. *273*, 7835–7842.

De Silva, I.U., McHugh, P.J., Clingen, P.H., and Hartley, J.A. (2000). Defining the roles of nucleotide excision repair and recombination in the repair of DNA interstrand cross-links in mammalian cells. Mol. Cell. Biol. *20*, 7980–7990.

D'Incalci, M., and Galmarini, C.M. (2010). A review of trabectedin (ET-743): a unique mechanism of action. Mol. Cancer Ther. *9*, 2157–2163.

D'Incalci, M., and Jimeno, J. (2003). Preclinical and clinical results with the natural marine product ET-743. Expert Opin. Investig. Drugs *12*, 1843–1853.

Dynan, W.S., and Tjian, R. (1983). The promoter-specific transcription factor Sp1 binds to upstream sequences in the SV40 early promoter. Cell *35*, 79–87.

Friedman, D., Hu, Z., Kolb, E.A., Gorfajn, B., and Scotto, K.W. (2002). Ecteinascidin-743 inhibits activated but not constitutive transcription. Cancer Res. *62*, 3377–3381.

Frit, P., Kwon, K., Coin, F., Auriol, J., Dubaele, S., Salles, B., and Egly, J.M. (2002). Transcriptional activators stimulate DNA repair. Mol. Cell *10*, 1391–1401.

García-Nieto, R., Manzanares, I., Cuevas, C., and Gago, F. (2000). Increased DNA binding specificity for antitumor ecteinascidin 743 through protein-DNA interactions? J. Med. Chem. *43*, 4367–4369.

Guirouilh-Barbat, J., Redon, C., and Pommier, Y. (2008). Transcription-coupled DNA double-strand breaks are mediated via the nucleotide excision repair and the Mre11-Rad50-Nbs1 complex. Mol. Biol. Cell *19*, 3969–3981.

Guirouilh-Barbat, J., Antony, S., and Pommier, Y. (2009). Zalypsis (PM00104) is a potent inducer of gamma-H2AX foci and reveals the importance of the

C ring of trabectedin for transcription-coupled repair inhibition. Mol. Cancer Ther. *8*, 2007–2014.

Huang, H., Zhu, L., Reid, B.R., Drobny, G.P., and Hopkins, P.B. (1995). Solution structure of a cisplatin-induced DNA interstrand cross-link. Science *270*, 1842–1845.

Jin, S., Gorfajn, B., Faircloth, G., and Scotto, K.W. (2000). Ecteinascidin 743, a transcription-targeted chemotherapeutic that inhibits MDR1 activation. Proc. Natl. Acad. Sci. USA *97*, 6775–6779.

Kelley, L.A., and Sternberg, M.J. (2009). Protein structure prediction on the Web: a case study using the Phyre server. Nat. Protoc. *4*, 363–371.

Koeppel, F., Poindessous, V., Lazar, V., Raymond, E., Sarasin, A., and Larsen, A.K. (2004). Irofulven cytotoxicity depends on transcription-coupled nucleotide excision repair and is correlated with XPG expression in solid tumor cells. Clin. Cancer Res. *10*, 5604–5613.

Kuraoka, I., Kobertz, W.R., Ariza, R.R., Biggerstaff, M., Essigmann, J.M., and Wood, R.D. (2000). Repair of an interstrand DNA cross-link initiated by ERCC1-XPF repair/recombination nuclease. J. Biol. Chem. *275*, 26632–26636.

Leal, J.F., García-Hernández, V., Moneo, V., Domingo, A., Bueren-Calabuig, J.A., Negri, A., Gago, F., Guillén-Navarro, M.J., Avilés, P., Cuevas, C., et al. (2009). Molecular pharmacology and antitumor activity of Zalypsis in several human cancer cell lines. Biochem. Pharmacol. *78*, 162–170.

Mathis, D.J., and Chambon, P. (1981). The SV40 early region TATA box is required for accurate in vitro initiation of transcription. Nature *290*, 310–315.

McHugh, P.J., Spanswick, V.J., and Hartley, J.A. (2001). Repair of DNA interstrand crosslinks: molecular mechanisms and clinical relevance. Lancet Oncol. *2*, 483–490.

Minuzzo, M., Marchini, S., Broggini, M., Faircloth, G., D'Incalci, M., and Mantovani, R. (2000). Interference of transcriptional activation by the antineoplastic drug ecteinascidin-743. Proc. Natl. Acad. Sci. USA *97*, 6780–6784.

Mocquet, V., Kropachev, K., Kolbanovskiy, M., Kolbanovskiy, A., Tapias, A., Cai, Y., Broyde, S., Geacintov, N.E., and Egly, J.M. (2007). The human DNA repair factor XPC-HR23B distinguishes stereoisomeric benzo[a]pyrenyl-DNA lesions. EMBO J. *26*, 2923–2932.

Mu, D., Bessho, T., Nechev, L.V., Chen, D.J., Harris, T.M., Hearst, J.E., and Sancar, A. (2000). DNA interstrand cross-links induce futile repair synthesis in mammalian cell extracts. Mol. Cell. Biol. *20*, 2446–2454.

Muniandy, P.A., Liu, J., Majumdar, A., Liu, S.T., and Seidman, M.M. (2010). DNA interstrand crosslink repair in mammalian cells: step by step. Crit. Rev. Biochem. Mol. Biol. *45*, 23–49.

Newman, M., Murray-Rust, J., Lally, J., Rudolf, J., Fadden, A., Knowles, P.P., White, M.F., and McDonald, N.Q. (2005). Structure of an XPF endonuclease with and without DNA suggests a model for substrate recognition. EMBO J. *24*, 895–905.

Niedernhofer, L.J., Odijk, H., Budzowska, M., van Drunen, E., Maas, A., Theil, A.F., de Wit, J., Jaspers, N.G., Beverloo, H.B., Hoeijmakers, J.H., and Kanaar, R. (2004). The structure-specific endonuclease Ercc1-Xpf is required to resolve DNA interstrand cross-link-induced double-strand breaks. Mol. Cell. Biol. *24*, 5776–5787.

Ocio, E.M., Maiso, P., Chen, X., Garayoa, M., Alvarez-Fernández, S., San-Segundo, L., Vilanova, D., López-Corral, L., Montero, J.C., Hernández-Iglesias, T., et al. (2009). Zalypsis: a novel marine-derived compound with potent antimyeloma activity that reveals high sensitivity of malignant plasma cells to DNA double-strand breaks. Blood *113*, 3781–3791.

Oku, N., Matsunaga, S., van Soest, R.W., and Fusetani, N. (2003). Renieramycin J, a highly cytotoxic tetrahydroisoquinoline alkaloid, from a marine sponge Neopetrosia sp. J. Nat. Prod. *66*, 1136–1139. Erratum: (2004). J. Nat. Prod. *67*, 526.

Poindessous, V., Koeppel, F., Raymond, E., Comisso, M., Waters, S.J., and Larsen, A.K. (2003). Marked activity of irofulven toward human carcinoma cells: comparison with cisplatin and ecteinascidin. Clin. Cancer Res. *9*, 2817–2825.

Pommier, Y., Kohlhagen, G., Bailly, C., Waring, M., Mazumder, A., and Kohn, K.W. (1996). DNA sequence- and structure-selective alkylation of guanine N2 in the DNA minor groove by ecteinascidin 743, a potent antitumor compound from the Caribbean tunicate *Ecteinascidia turbinata*. Biochemistry *35*, 13303–13309.

Rahn, J.J., Adair, G.M., and Nairn, R.S. (2010). Multiple roles of ERCC1-XPF in mammalian interstrand crosslink repair. Environ. Mol. Mutagen. *51*, 567–581.

Riedl, T., Hanaoka, F., and Egly, J.M. (2003). The comings and goings of nucleotide excision repair factors on damaged DNA. EMBO J. *22*, 5293–5303.

Rinehart, K.L., Holt, T.G., Fregeau, N.L., Keifer, P.A., Wilson, G.R., Perun, T.J., Jr., Sakai, R., Thompson, A.G., Stroh, J.G., Shield, L.S., et al. (1990). Bioactive compounds from aquatic and terrestrial sources. J. Nat. Prod. *53*, 771–792.

Sawadogo, M., and Roeder, R.G. (1985). Interaction of a gene-specific transcription factor with the adenovirus major late promoter upstream of the TATA box region. Cell *43*, 165–175.

Schinecker, T.M., Perlow, R.A., Broyde, S., Geacintov, N.E., and Scicchitano, D.A. (2003). Human RNA polymerase II is partially blocked by DNA adducts derived from tumorigenic benzo[c]phenanthrene diol epoxides: relating biological consequences to conformational preferences. Nucleic Acids Res. *31*, 6004–6015.

Scott, J.D., and Williams, R.M. (2002). Chemistry and biology of the tetrahydroisoquinoline antitumor antibiotics. Chem. Rev. *102*, 1669–1730.

Soares, D.G., Escargueil, A.E., Poindessous, V., Sarasin, A., de Gramont, A., Bonatto, D., Henriques, J.A., and Larsen, A.K. (2007). Replication and homologous recombination repair regulate DNA double-strand break formation by the antitumor alkylator ecteinascidin 743. Proc. Natl. Acad. Sci. USA *104*, 13062–13067.

Stehlikova, K., Kostrhunova, H., Kasparkova, J., and Brabec, V. (2002). DNA bending and unwinding due to the major 1,2-GG intrastrand cross-link formed by antitumor cis-diamminedichloroplatinum(II) are flanking-base independent. Nucleic Acids Res. *30*, 2894–2898.

Sydow, J.F., Brueckner, F., Cheung, A.C., Damsma, G.E., Dengl, S., Lehmann, E., Vassylyev, D., and Cramer, P. (2009). Structural basis of transcription: mismatch-specific fidelity mechanisms and paused RNA polymerase II with frayed RNA. Mol. Cell *34*, 710–721.

Takebayashi, Y., Pourquier, P., Zimonjic, D.B., Nakayama, K., Emmert, S., Ueda, T., Urasaki, Y., Kanzaki, A., Akiyama, S.I., Popescu, N., et al. (2001). Antiproliferative activity of ecteinascidin 743 is dependent upon transcription-coupled nucleotide-excision repair. Nat. Med. *7*, 961–966.

Tavecchio, M., Simone, M., Erba, E., Chiolo, I., Liberi, G., Foiani, M., D'Incalci, M., and Damia, G. (2008). Role of homologous recombination in trabectedin-induced DNA damage. Eur. J. Cancer *44*, 609–618.

Zawel, L., Kumar, K.P., and Reinberg, D. (1995). Recycling of the general transcription factors during RNA polymerase II transcription. Genes Dev. *9*, 1479–1490.

Zewail-Foote, M., and Hurley, L.H. (1999). Ecteinascidin 743: a minor groove alkylator that bends DNA toward the major groove. J. Med. Chem. *42*, 2493–2497.

Zewail-Foote, M., Li, V.S., Kohn, H., Bearss, D., Guzman, M., and Hurley, L.H. (2001). The inefficiency of incisions of ecteinascidin 743-DNA adducts by the UvrABC nuclease and the unique structural feature of the DNA adducts can be used to explain the repair-dependent toxicities of this antitumor agent. Chem. Biol. *8*, 1033–1049.